Journal of Water Resource and Protection, 2019, 11, 1090-1109
http://www.scirp.org/journal/jwarp
ISSN Online: 1945-3108
ISSN Print: 1945-3094

Groundwater Flow Modeling by Using the Permeability Induced by Satellite Lineaments in Discontinuous Aquifers and Semi-Arid Context: A Case Study of the Liptako Region (South-West of Niger)

Saidou Garba Inaytoulaye[1*], Youssouf Koussoube[2], Abdel Kader Hassane Saley[1], Issoufou Sandao[1], Paul Hayes[3], Boureima Ousmane[1]

[1]Department of Geology, Faculty of Science and Technology, Abdou Moumouni University, Niamey, Niger
[2]Department of Earth Sciences, Life and Earth Sciences Unit, Joseph Ki-Zerbo University, Ouagadougou, Burkina Faso
[3]International Aid Service of Niamey, Niger
Email: *isaidougarba@yahoo.fr, isaidougarba@gmail.com

How to cite this paper: Saidou, G.I., Koussoube, Y., Saley, A.K.H., Sandao, I., Hayes, P. and Ousmane, B. (2019) Groundwater Flow Modeling by Using the Permeability Induced by Satellite Lineaments in Discontinuous Aquifers and Semi-Arid Context: A Case Study of the Liptako Region (South-West of Niger). *Journal of Water Resource and Protection*, **11**, 1090-1109.
https://doi.org/10.4236/jwarp.2019.118064

Received: June 28, 2019
Accepted: August 27, 2019
Published: August 30, 2019

Abstract

The study area, located in the Liptako basement of Niger, faces a serious problem of drinking water supply in recent decades. This is linked to exponential population growth and reduced rainfall. The purpose of this study is to map fracture networks from Landsat 7 satellite imagery to identify major subterranean flow corridors in the area. The methodological approach based on the collection of data (Landsat 7 images, DEM/SRTM, flow, transmissivity, static level) and the geological and hydrogeological field reconnaissance and the processing of these data with the following software (ArcGis, Envi, Surfer and RStudio) The results of this study yielded that the number of satellite lineaments is 995, the preferred directions of these satellite lineament are: N0˚-10˚ (13%) and N90˚-100˚ (12%). On the hydrographic network, in situ, the most frequent fracture, vein and dike directions are: N90˚-100˚ (12%), N130˚-150˚ (11%), and N50˚-60˚ (10%). The structural domains identified probably correspond to the main corridors and reservoirs of underground flows. The values of the induced permeability are between 0.05×10^{-8} and 3.4×10^{-7} m/s. The permeability induced by satellite lineaments, which is strongly related to high fracturing densities and major water stream is involved in the hydrodynamic functioning of discontinuous aquifers in the study area.

Keywords

Satellite Image, Circulation Corridor, Induced Permeability, Hydrogeological Modeling, Tamou

1. Introduction

In basement areas, groundwater reservoirs are found mainly in fracture networks and alterations [1] [2]. Indeed, fracture networks are the main paths of underground flows in rocks [3]. In West Africa, several authors [1]-[8] and particularly in Niger, [9]-[14] were conducted on fracking to the hydrodynamic operation of discontinuous aquifers in the basement zone.

The study area consists of basement formations, is facing a significant migration of populations, from the northern part of the Tillaberi region (Ouallam), in search of a favorable climate. However, the infrastructures built by the Niger authorities during the 1000 boreholes campaign since the end of the 1970s, remain insufficient in face of strong population growth: 36,679 inhabitants in 1988 and 104,070 inhabitants in 2016 (according to the projections of INS, 2016). All this has led the rural population to use surface water during winter (marigots, rivers, koris), which are sensitive to possible anthropogenic pollution, cause of various waterborne diseases (cholera, dysentery, typhoid fever, poliomyelitis). During the dry season, these populations rely on groundwater using traditional wells [9]. These sheets, of limited extent, are highly dependent on rainfall and in most cases are exhausted before the return of the rains, sometimes cause the displacement of an entire village [12]. Thus, the lack of in-depth study on the implementation of the structures leads to a very high failure rate in the basement area and particularly in the commune of Tamou, where 45 boreholes were recorded out of a total of about 200 boreholes, about a quarter of a failure rate. In addition, even among the positive drillings, 56 drillings or 38% have a flow less than or equal to 1 m^3/h. Therefore, it seems urgent to undertake a thorough study for better exploitation of the water potential. This study aims specifically to: establish a map of linearity and induced permeability of the zone, make correlations between the induced permeability and the hydrogeological and hydrodynamic properties.

2. Materials and Methods

2.1. Study Site

Located in the department of Say, the study area is limited to the north by the urban community of Say, south-west by the borders of Burkina Faso and Benin, to the south by the Benin border, to the east by the Niger River and the rural commune of Kirtachi, and to the West by the rural commune of Gueladio (**Figure 1**). It covers an area of 5230 km^2, or 36.24% of the Say Department. The Niger River is the main permanent flowing stream in the area while Goroubi,

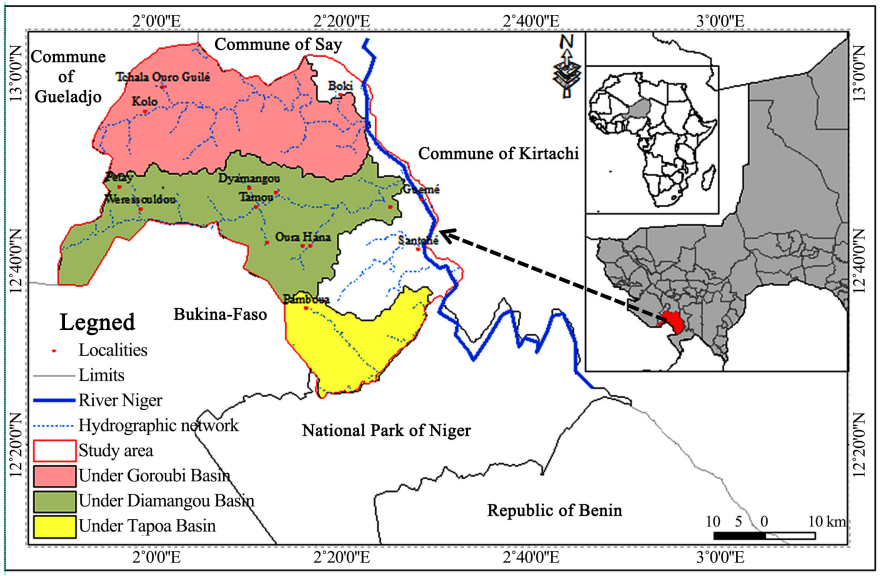

Figure 1. Location of the study area.

Diamangou and Tapoa are its tributaries. These tributaries also play an important role; they cover the eastern part of a sub-catchment basin of the Niger watershed, which has an outlet for the hydrometric station at Tondikwaré.

This zone straddles the Sahelian zone in the north where the rainfall varies from 400 to 600 mm per year and the Sahelo-Sudanian zone whose annual rainfall is greater than 600 mm. The rainy season runs from mid-May to October and the dry season prevails throughout the rest of the year. The average rainfall module calculated over the 1981-2016 period is 698 mm (National Meteorological Direction, 2017). Annual average temperature values range from 28˚C to 30.4˚C for the period 1961-2016.

The vegetal covers in the form of a mosaic of facies, is of tiger bush type on the battleship plateau, while on the glacis, it is rather organized agroforestry park largely dominated by Combretaceae [15].

The low relief is weakly wavy with altitudes between 170 m and 260 m. The highest elevations are located at the top of control hills and mounds in the study area.

Soils are ferruginous tropical on the sandy plateau and litho-regosols type on ferruginous cuirasses [16] and [17]. The soils encountered in the glacis are ferruginous types more or less leached while they are hydromorphic in the wetlands of the shallows and some temporary beds of ponds.

The main geological formations of the study area are divided into three large groups (**Figure 2**): a set of formations of the Birimian basement of Paleoproterozoic age 2300 - 2000 Ma, which takes the form of an alternation of granodioritic plutons [11] [18] and NW-SE oriented greenstone belts. Granodioritic plutons consist of granodiorite, quartz diorite and various granites; on the other hand, greenstone rocks consist of schists, conglomerates, metabasites and meta-ultrabasites.

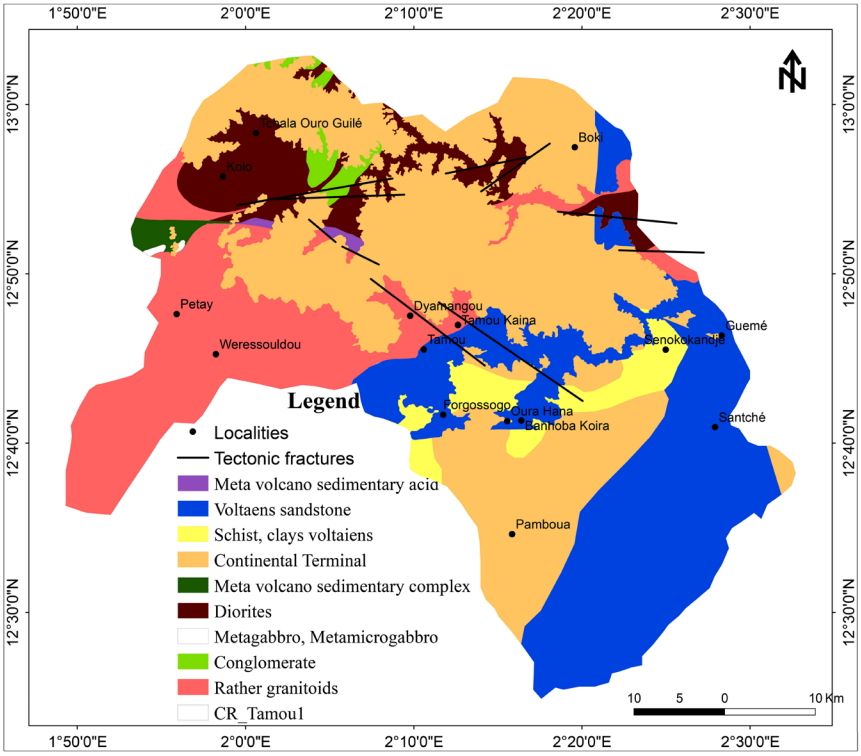

Figure 2. Geological map of the study area.

These formations are affected by more or less intense accidents which principal directions are: NW-SE, NE-SW, E-W and N-S [11].

The second subassembly consists of Infracambrian formations consist of volcanic rocks, consisting of arkosic sandstones, quartzitic sandstones and conglomerates.

Finally, the last set includes the Continental Terminal (CT3) and Quaternary formations: the sedimentary rocks of the CT3 consist mainly of fine to coarse clayey sandstones, sandy clay levels with several levels of ferruginous oolites which are discrepancies on the more or less kaolinized Birimian basement [9] [19]. Quaternary deposits correspond to sandy, alluvial, colluvial and lateritic mantle coverings.

The hydrogeological context is characterized by the presence of two types of aquifers: discontinuous aquifers (altered, fissured and fractured zones) and continuous aquifers encountered in sedimentary formations. Basement rocks are aquifers only at the level of the first 100 meters [20]. The overall drilling depth ranges from 20 m to 100 m with an average of 61.75 m and a standard deviation of 15.22 m. The values of the static levels are between 1.27 and 79.3.

2.2. Equipment

The material used in this study is composed of the following data and tools:

2.2.1. Data Used

- An extract of the GeoCover Circa 2000 mosaics (N30-10 and N30-15) of the October 2000 Landsat 7 satellite ETM + image downloaded from

http://www.zulu.nasa for the realization of the map of lineaments.

- A DEM 30 m resolution SRT image downloaded from http://dds.cr.usgs.gov/srtm/version2_1/SRTM3/Africa/
- The Liptako geological map (1/200,000) provided by the Ministry of Mine, the Kirtachi topographic map at a scale of 1/200,000, and the data sheets concerning 199 hydraulic boreholes are acquired at the Ministry of the hydraulic and sanitation and their partner.
- The documents used are mainly composed of thesis reports and reports on tectonic studies.

2.2.2. Tools

They are essentially composed of softwares:

- Envi 4.4 for the processing of satellite images;
- ArcGIS10.2.2 and Surfer for mapping watershed delineation, administrative boundaries, tracing of lineaments, mesh of study area, determination of lineament angles and lengths;
- Linwin and Oriana, for the directional rosette of Landsat images and the directional rosette for field structure measurements;
- RStudio for programming the computation of induced permeability and statistical calculations of hydrogeological and hydrodynamic parameters.

2.3. Methodology

The methodological approach is as follow:

2.3.1. Pretreatment of ETM + Sensors Images from LANDSAT 7 Satellite

The preliminary phase of satellite image processing consists of eliminating radiometric noise in the ETM + bands and correcting the geometric distortions in order to make them perfectly superimposable to the existing thematic maps (topographic, geological and photogeological maps), [3]. The Landsat 7 ETM + multiband image used in this study is an excerpt from a GeoCover mosaic image of October 2000. It has a geometric resolution of 30 m. It was resampled and merged to band 8 with a 15 m geometric resolution. It was then orthorectified, which makes it possible to reduce the size of the pixel to a square of 14.25 m of side (**Figure 3**). The Landsat 7 ETM + image comprise the following three spectral bands: 2 (green, visible), 4 (near infrared) and 7 (medium infrared), including a 4-7-2 RGB color composition to obtain an image in false colors quite easy to interpret. The image has been enhanced by Equalization to process contrast to maximize information.

2.3.2. Extraction of Lineaments

The processed image was introduced into the ArcMap system where the lineaments were manually extracted at a scale of 1:50,000. The analog plot was based on the natural signatures of visual fractures to the naked eye such as: geological contact, plant alignment; the rectilinear borders of the cornices of the lateritic

cuirasses, the contrasts of tone and texture. Figure 4 summarizes the different steps of the extraction of lineaments.

2.3.3. Control and Validation of the Lineament Map

The validation phase of the linear map is essential to judge the relevance of the applied method [3]. It comprises three approaches in this study: 1) a first one consisting in superimposing the road and topographic map on the lineament map in order to remove the lineaments relative to anthropic activities (roads,

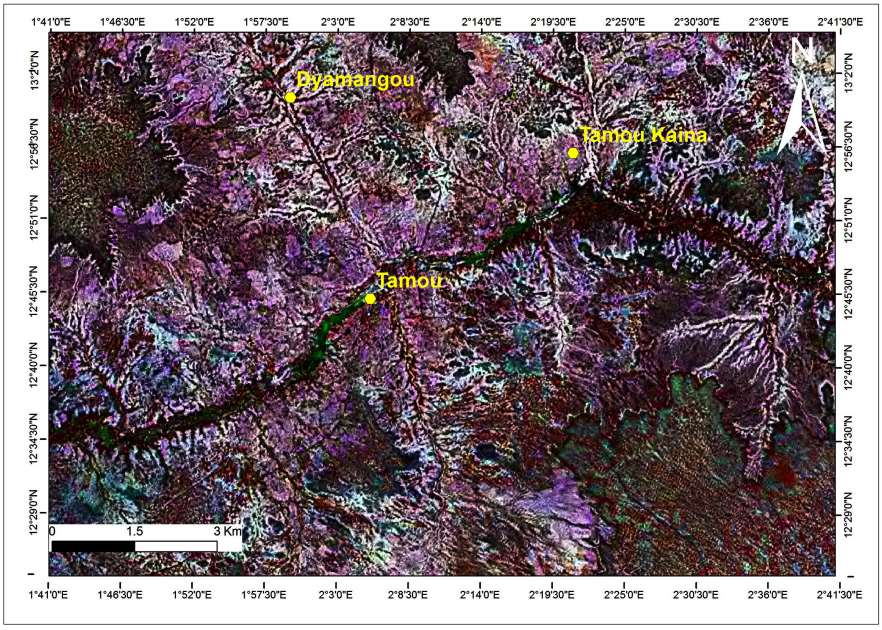

Figure 3. Landsat 7 ETM + image from October 2000 (false color RGB composite bands 4-7-2).

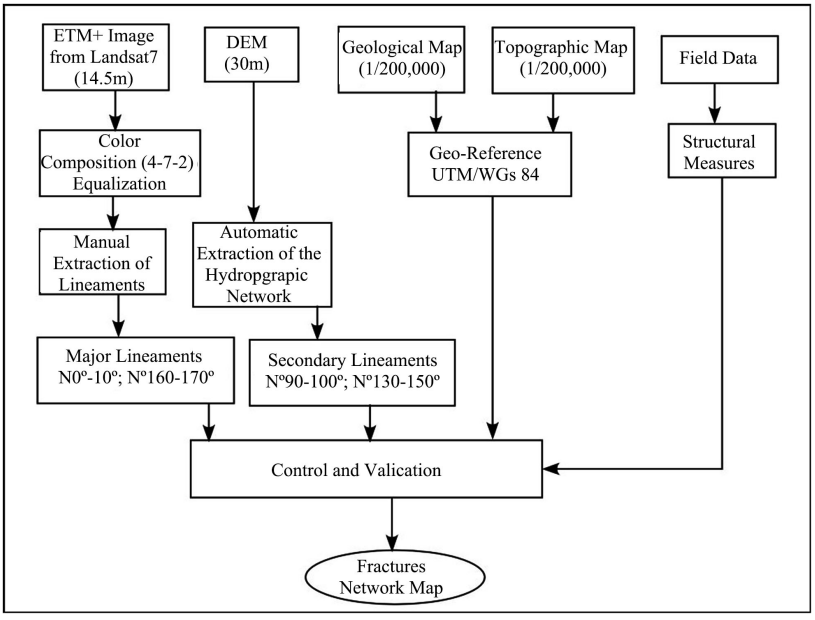

Figure 4. Steps in the realization of the fracturation map.

tracks, high voltages, etc.); 2) the second is based on the comparison between the major directions of the lineaments recorded on the Landsat image, the lineaments resulting from the hydrographic network and the microstructural field measurements. The lineaments of the hydrographic network come from an automatic extraction with the support DEM; 3) and finally the third is to verify the existence in the field of these lineaments from a geological and hydrogeological study.

2.4. Hydrogeological and Hydrodynamic Properties

The study of the relationships between the variables: transmissivities (T), specific flow rates (Qsp), and thicknesses of clay alterations (EA) required their transformation into bi-logarithmic. The correlation between T and Qsp highlights the geometry of fractures and their connectivity with drilling, while that between T and EA provides information on the productivity of aquifers.

2.5. Induced Permeability Calculation

According to the literature, there are two methods for modeling the underground flow in a fractured medium, namely the continuous model and the discrete model. The continuous model generates in the laboratory all the parameters coming into it while the discrete model uses data determined in the field, making it possible to find values similar to the reality of the field. Thus, the discrete model of Franciss (1970) was chosen as part of this work. For the calculation of induced permeability, several authors in West Africa including [4] and Koussoubé [5] in the basement of Burkina Faso, [1] [2] [7] [22] and [23] in Côte d'Ivoire have used the same model and have detailed and improved it. This parameter makes it possible to identify the major groundwater circulation axes. It is calculated according to the values of the characteristics of the boreholes measured in situ and the network of lineaments of the sector.

The application of the method of Franciss is based essentially on two assumptions defined as follows:

Fractures are assumed to be more or less vertical to simplify calculations. Thus, the study of the fracture density of the ETM + image by the directional rosette shows that these appear in their great majority vertical and/or subvertical;

- The thickness of the crushed area or the average gap between the two compartments of a surface fracture can be considered as an empirical linear function of the apparent length (L) of the megafracture. Thus, the application of this method requires the estimation of these two parameters C and Kf:

$$e = C \cdot L \rightarrow C = \frac{ei}{Li} \tag{1}$$

With,

e: thickness of the crushed area (m); corresponds to the difference between the depths of the first and last water inflow, or the length of the strainer in the case where the borehole has a single water inlet;

Li: length of the lineament (m);

C: empirical coefficient of proportionality. This coefficient was determined in the field by comparing the length and the opening of the hundreds of fractures measured in the field.

$$Kf = \frac{Ti}{ei}(\mathrm{m/s}) \tag{2}$$

With,

Ti: Transmissivity of the sector (m^2/s), the Transmissivity values data, from the drilling datasheets, were determined by the methods of Cooper-Jacob and Theis while using the method of the ascent. Indeed, the study area is very contrasted from the point of view of transmissivity. Thus, to standardize the medium, all the exceptional transmissivity values were suppressed; therefore 61 values were retained;

Kf: hydraulic conductivity of the sector (m/s), comparable to the apparent average permeability characterizing the entire studied surface. According to Franciss, the coefficient of permeability of a fracture is expressed by a symmetrical tensor of the second order and the tensor K which expresses the cumulative effect of several fractures is obtained by the sum of the tensors of each fracture contained in the space system considered. The modules of the vectors K are the maximum permeabilities ($K_{\max}$) and minimum permeabilities ($K_{\min}$) along the major axis and the short axis of the ellipse and form between them, an angle of 90˚, and are expressed according to the following formula:

$$K\begin{pmatrix}\max\\ \min\end{pmatrix} = \frac{1}{2}\left(K_{MN} + K_{\infty}\right) \pm \frac{1}{2}\sqrt{\left[\left(K_{MN} - K_{\infty}\right)^2 + 4K_{NO}^2\right]} \tag{3}$$

With,

K_{NN} and K_{∞}: permeabilities with respect to a North-South and East-West axis system. The average induced permeability of the base (K_{moy}) is determined by the following relation:

$$K_{moy} = 1/2 \cdot \left(K_{\max} + K_{\min}\right) \tag{4}$$

$$K_{\max} = 0.5 \cdot \frac{Kf}{D} \cdot CL\left(1 + \cos^2\lambda - \sin\lambda \cdot \cos\lambda\right) \tag{5}$$

$$K_{\min} = 0.5 \cdot \frac{Kf}{D} \cdot CL\left(1 - \cos^2\lambda + \sin\lambda \cdot \cos\lambda\right) \tag{6}$$

With,

$K_{\max}$ and $K_{\min}$ respectively represent the maximum and minimum principal permeabilities;

λ: indicates the direction of the permeability.

To complete this procedure, a laboratory study was done. This consists of meshing the sector's linear map to determine the fracturing variables. The mesh of the study area corresponds to 39 circles of 10,000 m of diameter of which each georeferenced circle is inscribed in a square of 10,000 m of side representing the

mesh. Thus, within each circle, the total number of lineaments, their length and their orientation relative to the North were determined. After determining the hydraulic conductivity (*Kf*) and the empirical proportionality coefficient (*C*) of the region, the values of the induced permeabilities are calculated. The application of the Franciss model makes it possible to integrate *Kf* and *C*, as well as the geometrical parameters of the lineaments to determine the values of the induced permeabilities of each mesh. The program established under the software R, by integrating the model of Franciss, makes it possible to calculate the induced permeabilities of the base.

3. Results

Figure 5 and Figure 6 represent respectively the fracturing maps of the satellite image and the hydrographic network.

3.1. Directional Distribution of Satellite Lineaments

The result of the directional rosette (Figure 7(a)) does not show a preferential direction. Nevertheless, it is found that the directional class N0˚-10˚ is the largest with a frequency of 13%, followed by the class N90˚-100˚ with a frequency of 7%. On the other hand, the other classes are very weak with frequencies varying between 3% and 6%.

Indeed, the statistical analysis of cumulative lengths shows that no class reaches a frequency of 10%, and the two main directions are: N0˚-10˚ (9%) and N160˚-170˚ (8%). The secondary directions are N10˚-20˚, N20˚-30˚, N30˚-40˚ and N140˚-150˚ with aoccurrence frequency of 7%. However, the directional class N0˚-10˚ remains the most dominant in fracture density.

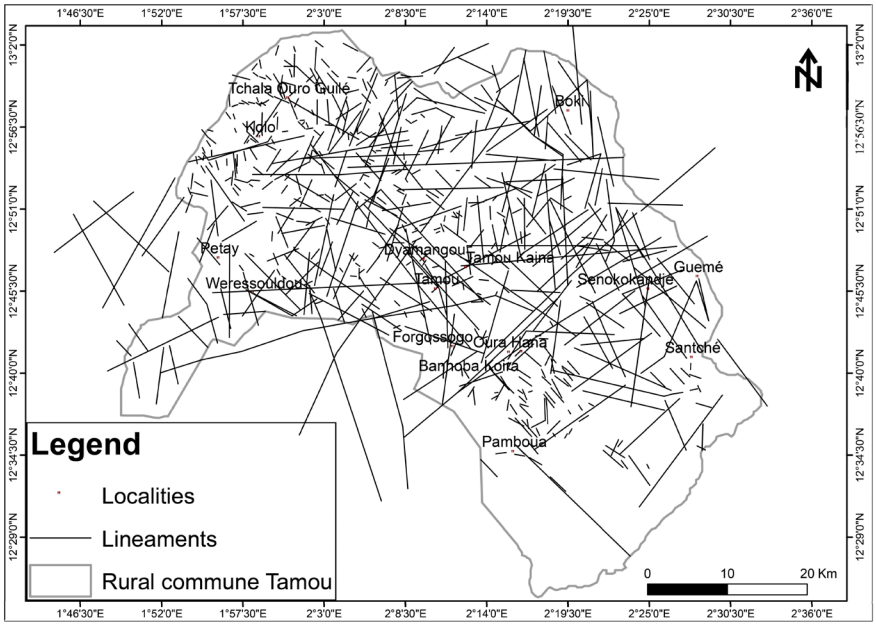

Figure 5. Map of the network of lineaments from the satellite image.

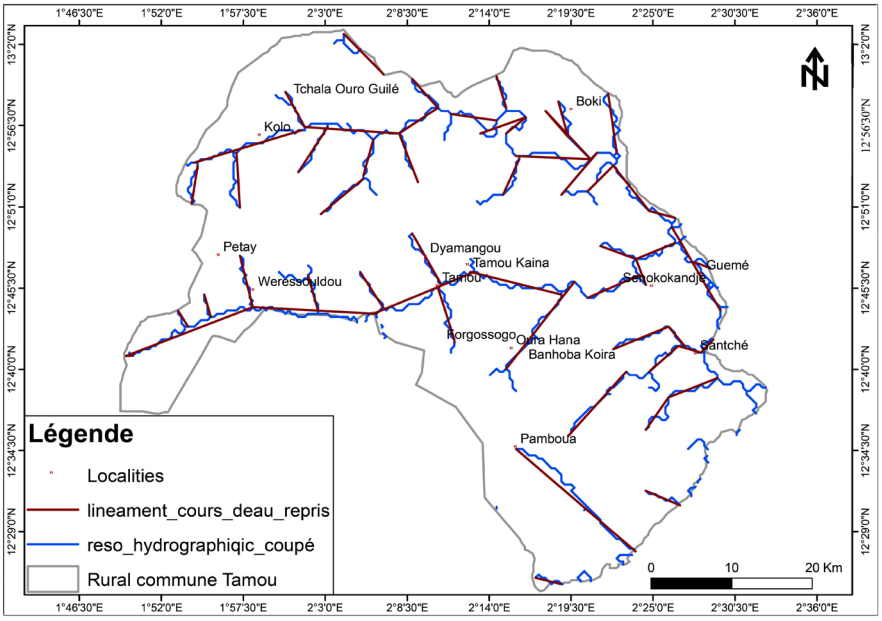

Figure 6. Map of fractures established from the hydrographic network.

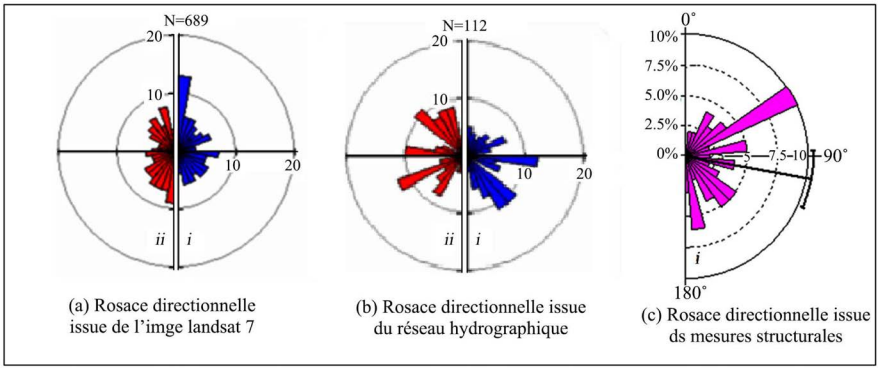

Figure 7. The different directional rosettes represent: (a) the Landsat 7 image; (b) the hydrographic network; (c) microstructural measurements (i: number of fractures, ii: cumulative lengths).

3.2. Distribution of Lineaments Drawn from the Hydrographic Network

Figure 7(b) shows essentially three main directions. It is: N90˚-100˚ (12%), N130˚-140˚ and N140˚-150˚ (11%) while N60˚-70˚ (7%), N110˚-120˚ and N160˚-170˚ (6%) represent the secondary classes. The statistical study of the cumulative lengths of lineaments also reveals three main major families which are: N60˚-70˚ (12%), N130˚-140˚ (11%) and N90˚-100˚ (10%) and to a lesser extent the directions N150˚-160˚ and N160˚-170˚ (9%), N30˚-40˚ and N140˚-150˚ (8%).

3.3. Directional Distribution of Fractures in the Field

The rosette on the structural data (fractures, quartz veins and pegmatite) found in the field (Figure 7(c)), shows that the frequency direction of the fractures is

N50˚-60˚ with a frequency of 10%, seconded more or less direction N160˚-170˚ with a frequency of 6.5%.

3.4. Hydrogeological Field Study

The hydrogeological verification phase was conducted in several villages spread over the area of the study area. Various species of vegetation: tree, shrub and sub-shrub were observed. Among the plant species, there are *Lannea microcarpum* and *Parkia biglobosa* (Nere) to Alambare, Moli Haoussa, and Pamboua. As shrubby and sub-shrubby plant species, the type of *Diospyros mespiliformis* and *Piliostigma reticulatum* has been identified. This category of plants is widespread throughout the area namely to Diango, Kotaki, Dar Salam, Kobouri. All these plants are hydrophilic and are good indicators of the presence of groundwater. The termite mounds (*Macrotermes bellicossus* and *Macrotermes subhalinus*) have also been observed in many villages, including BabobaKoira and Tondobanda. These results are consistent with those found by [24], in the Bidi watershed, Yatenga province (Burkina Faso).

3.5. Synthesis of Structural Mapping

The synthesis of the results obtained from the various supports (**Figure 7**) underlines the directions N0˚-10˚ (13%), N90˚-100˚ (12%), N130˚-140˚ and N140˚-150˚ (11%), N50˚-60˚ (10%) are most dominant followed by directions N60˚-70˚ and N160˚-N170˚ (7%), N110˚-120˚ and N160˚-170˚ (6%), and N140˚-150˚ (5%); while the main directions of cumulative lengths are N60˚-70˚ (12%), N130˚-140˚ (11%) and N90˚-100˚ (10%).

3.6. Hydrodynamic Properties of Aquifers

3.6.1. Transmissivity

The values of Transmissivities vary from 1.30×10^{-05} to 2.20×10^{-03} m^2/s, with an average of 2.28×10^{-04} m^2/s and a standard deviation of 3.36×10^{-04} m^2/s. **Figure 8** shows that transmissivities are relatively low in the study area with the exception of the northeastern part, which records values greater than 5 m/h.

3.6.2. Relationship between Transmissivities and Specific Flows

The correlation between transmissivities and specific flows provides information on the hydraulic properties of reservoirs [25]. **Figure 9** shows that the statistical test is satisfactory between the two variables with a correlation coefficient of about $R^2 = 0.81$; thus the relation linking these two parameters is linear and can be written in the following way:

$$\ln(Qsp) = 0.8316\ln(T) - 8.8096 \quad \text{et} \quad R^2 = 0.81 \tag{7}$$

3.6.3. Thickness Weathered and Clayer Zone

The thicknesses of saprolitein the study area (**Table 1**) can be classified into five groups according to the International Committee of Hydraulic Studies (CIEH). Strong and middle classes occupy more than 72% (**Table 1**). Indeed, the rela-

tionship between the transmissivities and the thicknesses of clay alterations shows an insignificant correlation (Figure 10).

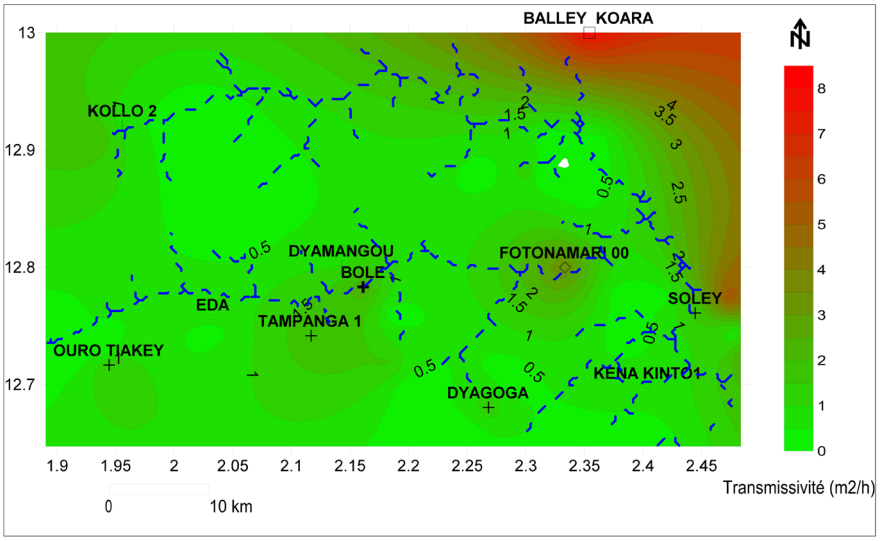

Figure 8. Spatial distribution of the transmissivity of the study area.

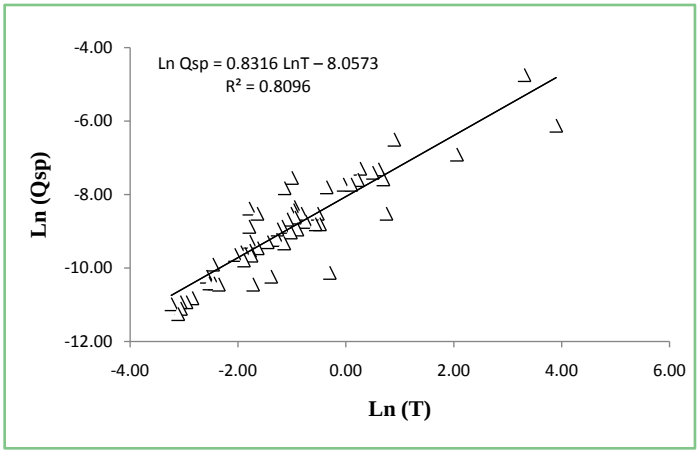

Figure 9. Relationship between transmissivity and specific flow.

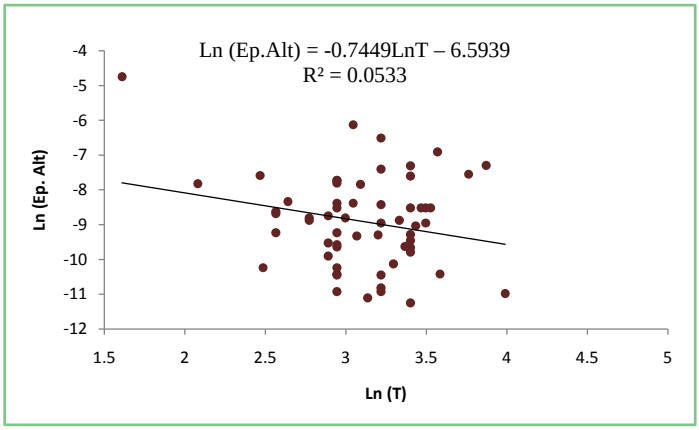

Figure 10. Relationship between transmissivity and the alteration thickness.

Table 1. Classification of alteration thicknesses according to the International Committee of Hydraulic Studies.

Classes	Very low	Low	Middle	Strong	Very strong
Thicknesses of saprolite	<10 m	10 - 15 m	15 - 25 m	25 - 40 m	40 - 70 m
Number (n = 117)	5	16	45	40	11
Percentage	4.27	13.68	38.46	34.19	9.40

3.7. Induced Permeability

For this model, the hydraulic conductivity and the coefficient of proportionality were obtained as follows:

✓ Hydraulic conductivity

$$Kf\left(\mathrm{m/s}\right)=\sum\frac{Ti}{ei}=\frac{3.14\mathrm{E}-01}{33881.9}=9.25\times10^{-6} \quad (8)$$

The value of Kf is acceptable because it belongs to the range of known values which vary between 10^{-8} and 10^{-4} m/s for the crystalline formations of West Africa [26].

✓ Coefficient of proportionality (see Equation (1), in the Methods Section)

$e = 28$ cm

$L = 5000$ cm

$C = e/L = 5.6 \times 10^{-3}$

This value is of the same order of magnitude as those found by [4] in Burkina Faso, and Côte d'Ivoire by [1] [7] [22] and [27].

The average permeability (k-avg) was chosen for this work. It ranges from 0.05×10^{-8} to 3.4×10^{-7} m^2/s with an average of 1.46×10^{-7} m^2/s and a standard deviation of 1.12×10^{-7} m^2/s. The analysis in **Figure 11** shows that the induced permeability values are reasonable for the study area which is a basement area. Thus, this same figure also shows that these values are in the same orders of magnitude as those found by [5] in Burkina Faso and [2] in Côte d'Ivoire.

Figure 12 shows the spatial distribution of the induced permeability as well as the major groundwater circulation axes. The identification of the groundwater circulation corridors was carried out by superimposing the map of spatial variation of the permeability and the density of drainage in the same plane. However, **Figure 12** shows the corridors where the circulation of groundwater is average or relatively large. The main directions are:

✓ A large axis with very high N-S to subvertical permeability that goes from SidiKoira, BaleyKoira to Boki areas;

✓ Another major axis oriented W-E;

✓ An axis oriented NE-SW that goes from BahobaKoira via TankoundéSékou-Kabé to Sénokokondjé.

Nevertheless, we can notice that the permeability is very low in the extreme northwestern and southwestern parts of the study area.

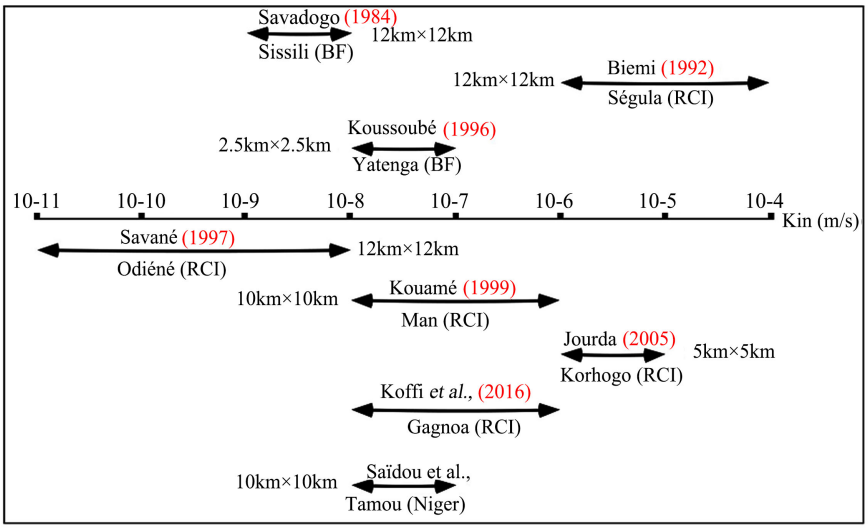

Figure 11. Comparative scale of induced permeabilities calculated in West Africa.

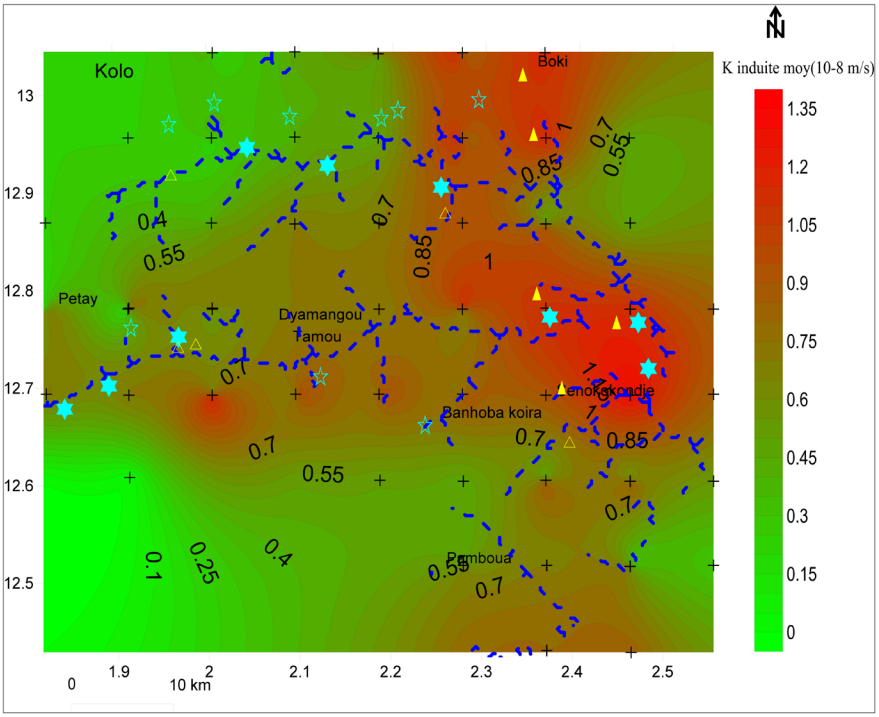

Figure 12. Map of the groundwater circulation corridors: triangle full: strong flows; empty triangles: low flow rates; solid stars: weak NS; empty stars: high NS.

Relationship between induced permeability and hydrogeological properties

A correlation matrix (Table 2) was made between the induced permeability and hydrogeological parameters. Table 2 shows the correlated variables, namely: K-T (0.97), Q-Qsp (0.85), Q-K (0.71) and Qsp-T (0.65).

The correlation of these parameters highlights their intervention in the operation and productivity of the boreholes in the study area.

Table 2. Correlation matrix.

Variables	NS	Q	S	Qsp	T	K	Ki	TD
NS	1							
Q	−0.09	1						
S	−0.19	−0.25	1					
Qsp	−0.03	0.85	−0.31	1				
T	−0.08	0.82	−0.32	0.65	1			
K	−0.08	0.71	−0.21	0.51	0.97	1		
Ki	−0.06	−0.03	0.2	0.02	−0.03	−0.01	1	
TD	0.19	−0.19	0.57	−0.2	−0.28	−0.25	−0.05	1

NS: static level; Q: flow rate; S: storage coefficient; Qsp: specific flow; K: permeability; Ki: induced permeability; TD: total depth.

4. Discussion

The modeling of the preferential axes of underground flow by the method of Franciss is based on the linear network satellite with a circle diameter of 10 km. Thus, in the study area, the directional distribution of lineaments revealed four principal directions: N0˚-10˚, N90˚-100˚, N130˚-150˚ and N50˚-60˚. To these main directions are added the secondary directions which are: N60˚-70˚ (7%), N110-120˚ and N160˚-170˚ (6%). Nevertheless, the direction N0-10˚ is the most dominant with 13% frequency. Indeed, this family has been found by several authors who have worked in similar areas: in Cote d'Ivoire [7] [8], Benin [28], and Niger [13]. It was also found in Burkina Faso in the region of Bidi/Yatenga [5] on type C lineaments (alignments of lateritic cuirass cornices). These tectonic accidents mainly affect the Birimian basement and are found in the extreme west of the study area, particularly towards Petay and Fanta Foulbé in the granodiorite. On the other hand, according to [28], the direction N0˚-10˚ which is the most important and the most outlined in the study area (North Benin) corresponds to the pan-African orientation of the tectono-metamorphic deformation.

The direction N90˚-100˚ is the second direction in terms of frequency after that of N0˚-10˚ in the zone of Tamou. This direction is much more remarkable on the lineaments of the hydrographic network characterizing the major direction of the rivers. It is superimposed perfectly with the satellite lineaments, so these lineaments correspond to fractures that follow the surface waters. This result is similar to the work of [8], carried out in the basement zone of Abidjan and [29] in the western part of Cote d'Ivoire.

The N50˚-60˚ directional class, which is one of the dominant directions observed in the field, is mainly found in the Goroubi sector where the rugged substratum is abundantly exposed. The accident mainly affected the outcrop of granodiorite formations. This direction belongs to the NE-SW orientation which also corresponds to the Eburnean direction.

The presence of active vegetation (tree species, shrubs and sub-shrubs) at the lineaments, confirm that the latter correspond to fractures. Consequently, these fractures represent corridors where the water reserve allows the good growth of plant species [30]. Thus, the remarkable alignment of termite mound buildings underlines fracture [4].

These results probably show that the dominant directional classes are the longest on the scale of 1/50,000 with the WGS 84 Repository/UTM, zone N31 for the ETM + image of LANDSAT 7. As the class N0˚-10˚ is the more important cumulative length. Therefore, there is good agreement in number and length in the preferential classes listed above; it is to be supposed that these directions are the most productive in this region. Thus, the model uses these lineaments to characterize the underground flow, while considering them as vertical and permeable fractures.

The values of the induced permeability of the study area vary between 0.05×10^{-8} and 3.4×10^{-7} m/s for squared meshes of 10 km. These values are higher than those found by [4] in Sissili and [22], in Odiéné, nevertheless, they are lower than the results found by [1] in Séguéla and [7] in Korhogo in Côte d'Ivoire (for mesh respectively of 12 km and 5 km side). The observed difference between these results perhaps explained by the fact that the fracturing map obtained by each author differs from one region to another [31] according to the tectonic history of the area and depending on the types of rocks encountered. A zone dominated by green rocks, does not react in the same way to constraints, as in a granitoid grain more or less coarse. In addition, it can be observed, as Savadogo pointed out in 1984, the smaller the mesh, the more the induced permeabilities are close to the true permeabilities. Indeed, the induced permeabilities are even greater than the meshes are small.

Figure 12 shows the spatial distribution of permeability induced in the study area. It highlights three major directions: N-S, E-W and NE-SW which probably correspond to the preferred directions of fracture networks. These axes of strong induced permeabilities constitute groundwater recharge zones in the study area. In addition, these main directions were also found by [11] in the Liptako basement. These directions of flow could coincide with the Euclidean fractures which correspond to the tectono-metamorphic event whose formations are dated 2, 4 and 1, 6 Ga (Yace, 1984 in [18]). Moreover, these directional axes have been superimposed on the hydrographic network, and there is a perfect concordance between these major axes of strong induced permeabilities and superficial streams. As a result, surface water supplies groundwater reservoirs through open fractures. This confirms the low NS drilling (solid star) that are located near water stream (water table depth < 6 m). Thus, the majority of structures with low water table are located in areas with medium and high induced permeability (**Figure 12**). The result of this study is in line with the work of [1] and [7], conducted in the bedrock of Côte d'Ivoire. However, **Figure 12** also shows strong permeabilities induced in the areas of Boki, BaleyKoira, Senokokondje. This

confirms the large flows (solid triangle) recorded in these villages which reach respectively 5.14 m^3/h, 5.14 m^3/h and 15 m^3/h. This result is similar to the work of [28], carried out in the Benin basement. In the NW extreme part of the study area, low values of induced permeabilities were recorded, confirming the low flow observed in the villages of Kolo, Tchala Ouro Guilé, Diango. These flow rates are respectively: 1.44 m^3/h, 1.07 m^3/h and 1.2 m^3/h. This low permeability could be due to a low fracturing density and where the fractures are relatively less open and are not interconnected.

Finally, from the results in **Table 2** there is no direct relationship between the induced permeability, the hydrogeological and the hydrodynamic parameters of the aquifers in this study. This could be due to the very low values of induced permeability recorded in the basement area.

5. Conclusion

Remote sensing combined with GIS is an essential technique for processing satellite images in order to map the fracture network. The latter made it possible to identify the preferential classes of major fracture and mega-fracture directions. Linear support served as databases to identify major underground flow axes: N-S, E-W and NE-SW, through the method of Franciss. This model yielded reasonable induced permeability results in the basement area. In addition, the groundwater circulation corridors coincide with the hydrographic network, which proves that parts of the aquifers are fed by surface water through drainage. However, this study confirms that the induced permeability does not directly affect the productivity of an aquifer in a fractured environment but is related to the density of the fractures (open and interconnected), to the flow rate and water table.

Acknowledgements

The authors thank very warmly and express their gratitude to the Non Governmental Organization: International Aid Service (IAS) Niger for the financial, material and human support it provided for the smooth running of this study. We also thank the Ministry of Hydraulics and Sanitation of Niger, Abdou Moumouni University (Niger) and Joseph Ki-Zerbo University (Burkina Faso) for their various contributions.

Conflicts of Interest

The authors declare no conflicts of interest regarding the publication of this paper.

References

[1] Biémi, J. (1992) Contribution to the Geological, Hydrogeological and Remote Sensing Study of Sub-Saharan Basins of the Precambrian Basement of West Africa: Hydrostructural, Hydrodynamic, Hydrochemical and Isotopic of Discontinuous Aqui-

fers of Furrows and Granitic Areas of the High Marahoué (Cote d'Ivoire). PhD Thesis, University of Natio-Cote d'Ivoire, Abidjan, 493 p.

[2] Kouamé, K.F. (1999) Hydrogeology of Discontinuous Aquifers in the Semi-Mountainous Region of Man-Danane (Western Cote d'Ivoire). Contribution of Satellite Imagery, Statistical and Fractal Data to the Development of a Spatially Referenced Hydrogeological Information System. PhD Thesis, Univ. Cocody-Abidjan, Abidjan, 194 p.

[3] Youan, T.M., Lasm, T., Jourda, J.P., Kouamé, K.E. and Razack, M. (2008) Mapping of Geological Accidents by Landsat 7 ETM + Satellite Imagery and Analysis of Precambrian Basement Fracture Networks of the Bondoukou Region (North-East of Cote d'Ivoire). *Remote Sensing Review*, **8**, 119-135.

[4] Savadogo, A.N. (1984) Geology and Hydrogeology of the Crystalline Basement of Upper Volta. Study of the Sissili Watershed Region. Thèse de Doctorates-Sciences, Univ. Scientifique et médicales de Grenoble, Grenoble, 340 p.

[5] Koussoubé, Y. (1996) Hydrogeology in Crystalline Basement Medium of Burkina Faso. Case of the Bidi Basin Watershed (Yatenga Province). PhD Thesis, Univ. Cheikh AntaDiop, Dakar, 210 p.

[6] Saley, M.B. (2003) Thematic Mapping of Fissure Aquifers for the Assessment of Water Resources. Implementation of a New Method of Extraction of Image Discontinuities and SIHRS for the Semi-Mountainous Region of Man Nord-Ouest of Côte d'Ivoire. PhD Thesis, University of Cocody-Abidjan, Abidjan, 209 p.

[7] Jourda, J.P.R. (2005) Methodology for Application of Remote Sensing and Geographic Information System Techniques to the Study of Fissured Aquifers in West Africa. Concept of Space Hydrotechnics: Case of the Test Areas of Côte d'Ivoire. PhD Thesis, Natural Sciences University of Cocody, Cocody, 429 p.

[8] Koffi, A.S., Ait, F.A., Elbelriti, H., El Gasmi, E. and Houssine (2013) Extraction by Remote Sensing of Major Fracture Networks from the Landsat Image of the Abidjan Region in Côte d'Ivoire. *Science Lib Editions Mersenne*, **5**, 20 p.

[9] Ousmane, B. (1988) Geochemical and Isotopic Study of Basement Aquifers of the Sahelian Belt of Niger (Liptako, South Maradi, Zinder East). Doctoral Thesis, University of Niamey, Niamey, 441 p.

[10] Girard, P. (1993) Isotopic Techniques (15N, 18O) Application to the Study of the Plains of Alterites and the Fractured Base of West Africa. Case Study: Western Niger. PhD Thesis, University of Québec, Montréal, 154 p.

[11] Soumaila, A. and Konate, M. (2005) Caractérisation de la déformation dans la ceinture birimienne (paléoprotérozoïque) de Diagorou-Darbani (Liptako nigérien, Afrique de l'Ouest). *Africa Geoscience Review*, **13**, 161-178.

[12] Abdou Babaye, M.S. (2012) Assessment of Groundwater Resources in the Dargol Basin (Liptako-Niger). PhD Thesis, University of Liège-Belgium and Abdou Moumouni University of Niamey-Niger, Niamey, 265 p.

[13] Illias, A., Abdou, B.M.S., Sandao, I., Saley, M.B. and Ousmane, B. (2018) Contribution of ETM + and Digital Terrain Model (DTM) Imagery to Mountain Fracture Mapping: Timia Area (Massif de l'Air). *European Scientific Journal*, **14**, 19 p.

[14] Abdou, A.I., Konaté, M. and Ousmane, B. (2018) Lineamentary and Structural Cartography of Iullemmenden Basin of Dosso Region (South-West of Niger). *International Journal of Science and Research*, **7**, 9.

[15] Ambouta, K. (1984) Contribution to the Edaphology of the Western Tiger Bush Nigerien. PhD Thesis, University of Nancy I, Nancy, 116 p.

[16] Gavaud, M. (1965) Pedology of Western Niger. ORSTOM—MDR Dakar Center, Dakar, 573 p.

[17] Guéro, Y. (2006) Soil Characterization and Assessment of Edaphic Resources: Keita, Tamaské, Ibohamane, Kalfou, Bambey, Tahoua 1 and 2 Communes (Tahoua Region), Kourtey, Ouallam and Simiri (Tillaberi Region). Report on Preliminary Characterization Studies of Initial State A0, 22 p.

[18] Soumaila, A. (2000) Structural, Petrographic and Geochemical Study of the Diagorou-Darbani Belt, Liptako, Western Niger (West Africa). PhD Thesis, University of Franche-Comté, Besançon, 253 p.

[19] Guero, A. (2003) Study of the Hydraulic Relations between the Different Aquifers of the Sedimentary Complex of the South-Western Border of the Iullemmeden Basin (Niger): Geochemical and Hydrodynamic Approaches. PhD Thesis, University Paris-Sud 11-Orsay, Paris, 265 p.

[20] BoubacarHassane, A. (2010) Superficial and Deep Aquifer and Urban Pollution in Africa: Case of the Urban Community of Niamey (Niger). PhD Thesis, Abdou Moumouni University of Niamey, Niamey, 249 p.

[21] Franciss, F.O. (1970) Contribution to the Study of the Movement of Water through Rocks. Thesis Doctor Engineer, University Grenoble I, Saint-Martin-d'Hères, 112 p.

[22] Savané, I. (1997) Contribution to the Geological and Hydrogeological Study of Discontinuous Aquifers of the Crystalline Basement of Odienne (North-West of Côte d'Ivoire). Contribution of Remote Sensing and a Hydrogeological Information System with Spatial Reference. Doctoral Thesis in Natural Sciences Univ., Cocody, 410 p.

[23] Savané, I., Goze, B.B.Q. and Hugh, J.G.W.J.N. (1997) Assessment of the Productivity of Basement Structures by the Study of Fractures and GIS in the Northwestern Region of Côte d'Ivoire. Hard Rock Hydrosystems (Proceedings of Rabat Symposium S2, May 1997). IAHS Publ. No. 241, 9 p.

[24] Koussoubé, Y., Savadogo, A.N. and Nakolendoussé, S. (2003) The Different Signatures of Crystalline Basement Fractures in the Sahelo-Sudanese Zone of Burkina Faso (Bidi Basin, Province of Yatenga). 10 p.

[25] Kouassi, E.A., Koffi, Y.B., Kouassi, A.M., Soro, G., Soro, N. and Biemi, J. (2013) Hydrodynamic Functioning of Discontinuous Aquifers in the Abidjan-Agboville Region (Southern Cote d'Ivoire). *International Journal of Geography and Geology*, **2**, 52-69.

[26] Kouassi, A.M., Okaingni, J.C., Kouakou, K.E. and Biémi, J. (2013) Evaluation of the Hydraulic Properties of Crystalline and Crystallophillic Basement Aquifers: Case of N'zi-Comoé Region (East Center of Cote d'Ivoire). *International Journal of Innovation and Applied Studies*, **2**, 11 p.

[27] Emile, A.A., Damien, A.K., Abaka, B.H.M., Alain, N.K., Aimé, K., Hélène, B.K., Dibi, H.N., René, T. and Moumtaz, R. (2014) Application of Remote Sensing and Multicriteria Analysis Methods to the Study of Spatial Variability of Groundwater Potential of a Basement Aquifer of a Humid Tropical Region of West Africa: Case of Bongouanou Department, Eastern Côte d'Ivoire.

[28] Akokponhoué, B.H., Yalo, N., Lasm, T., Youan, T.M., Alassane, A., Kouamé, J.K., Akokponhoué, N.Y., Hounton, C.C. and Suanon, F. (2017) Contribution of Remote Sensing to the Structural Mapping of Aquifers with Large Water Flows in the Crystalline Hard Rock in the Department of Dongo (North-West of Benin). *International Journal of Emerging Technology and Advanced Engineering*, 12.

[29] Oularé, S., Kouamé, A.K., Saley, M.B., Ake, G.E., Kouassi, M.A., Adon, G.C., Kouamé,

F.K. and Therrien, R. (2016) Estimation of the Hydraulic Conductivity of Discrete Fracture Network Zones from Hydraulic Loads: Application to the Basin N'zo Slope (Western Cote d'Ivoire). *Journal of Water Science*, **7**, 24 p.

[30] Kouakou, K.E.G., Dosso, L., Kouamé, L.N., Sombo, A.P. and Sombo, B.C. (2015) Contribution of Electrical Resistivity Methods to the Search for Water in Crystalline Media: Case of Yakassé-Attobrou and Abié, Mé Region, Cote d'Ivoire. *Revue Ivoirienne des Sciences et Technologie*, **26**, 194-211.

[31] Koffi, K.M.,Yao, T., Mobio, A. and Oga, Y.M.S. (2016) Contribution of the Muticritère Analysis to the Mapping of Areas Favorable to the Implantation of Boreholes in the Gagnoa Region (Center-West of Côte d'Ivoire). *Geo-Eco-Trop*, **40**, 327-344.